CHARACTERIZING THE FRACTURE OF TANTALUM NITRIDE FILMS ON AlN SUBSTRATES THROUGH FILM THICKNESS EFFECTS

N. R. MOODY, D. MEDLIN, and D. P. NORWOOD*
Sandia National Laboratories, Livermore, CA 94551-0969
*Sandia National Laboratories, Albuquerque, NM, 87185

ABSTRACT

In this study, nanoindentation and nanoscratch testing were combined with transmission electron microscopy to establish the relationship between structure, properties, and fracture resistance of thin tantalum nitride resistor films on aluminum nitride substrates. The films were sputter-deposited to thicknesses of 160, 440, and 500 nm. Nanoindentation was used to determine mechanical properties while indentation fracture and nanoscratch tests were used to measure interfacial fracture energies. These tests showed that the measured elastic moduli of all films were independent of indenter depth and approximately equal to the value measured for the aluminum nitride substrates. They also showed that measured hardness values increased with film thickness. More importantly, the fracture energies measured in indentation fracture and nanoscratch tests were essentially equal and independent of film thickness. These results showed that tantalum nitride films and aluminum nitride substrates behaved in an inherently brittle manner. They further showed that fracture was localized along the interface suggesting that adhesion was controlled by the nature of bonding across the interface plane.

KEYWORDS

Nanoindentation, indentation fracture, nanoscratch fracture, tantalum nitride films, aluminum nitride substrates.

INTRODUCTION

Thin films are used in many applications where resistance to abrasion, corrosion, permeation and oxidation, as well as special magnetic and dielectric properties are needed to ensure performance and reliability. (Mittal, 1976) These films range from native oxide passivating layers to exotic films deposited for unique properties. In all these applications, performance can degrade over time and be completely lost when the films fail. As a consequence, a number of techniques have been developed to measure resistance to fracture. (Mittal, 1976; Rickersby, 1988) Two tests that yield reasonable estimates for fracture energies of films in the as-deposited configuration are indentation fracture and nanoscratch. (Venkataraman et al., 1993;Weppelmann et al., 1994; Evans and Hutchinson, 1984)

Of particular interest are thin tantalum nitride films. These films are used extensively in microelectronic applications such as resistors and capacitors because of their long term stability and low thermal coefficient of resistance. (Au et al., 1990) Although these films are strong heat generators, they exhibit no changes in structure or composition of the interface with aluminum oxide substrates that degrade performance or reliability. However, the use of high power density components is driving a move to replace aluminum oxide with aluminum nitride for

greater heat transfer. (Garrou, 1994; Palmer, 1994) This replacement substrate creates concern as elevated temperature exposure and long-term operation could induce detrimental changes along the thin film interface not observed in aluminum oxide devices. Nanoindentation (Doerner and Nix, 1986; Nix, 1989) and nanoscratch testing (Wu, 1991; Venkataraman et al. 1993) were therefore combined with transmission electron microscopy in this study to establish the relationship between the structure, properties, and fracture resistance of thin tantalum nitride films on aluminum nitride substrates.

MATERIALS AND PROCEDURE

In this study, thin tantalum nitride films were reactively sputtered onto polished polycrystalline aluminum nitride substrates using a d. c. magnetron sputtering unit. The substrates were prepared by cleaning in detergent, soaking in trichloroethane, and rinsing in methanol. They were then heated to 850°C in air for one hour to produce a surface oxide. After air-heating, they were transfered to a deposition chamber and heated to 170°C in vacuum for two hours to drive off moisture. Cleaning was completed with an RF backsputter for 15 seconds to remove contaminants from the surface of the oxide layer. With a vacuum maintained to less than $1.3x10^{-5}$ Pa (10^{-7} torr), the films were deposited on the substrates using a tantalum target, argon as a carrier gas, and controlled additions of nitrogen to form Ta_2N. Deposition was at a rate of 0.3 nm/s onto the surfaces of the aluminum nitride substrates to give nominal film thicknesses of 160, 440, and 500 nm. Profilometry and TEM cross-sections were then used to confirm film thicknesses.

The elastic moduli of the as-sputtered films were determined from a series of indentations employing an indentation test system developed by Nano Instruments, Inc. (Doerner and Nix, 1986; Oliver and Pharr, 1992) The tests were conducted at a constant loading rate of 300 µN/s to depths ranging from 20 to 600 nm using a Berkovich indenter. Indentation loads and corresponding depths were recorded continuously throughout each test. The contact areas for one-half of the indentations on the 160-nm-thick film were measured directly in a JEOL 840 SEM. These areas were used to determine the elastic modulus and hardness as well as to verify the applicability of the indenter shape function established from earlier tests on single crystal aluminum, fused silica, and thin tantalum nitride and aluminum films. From this relationship the contact areas for all other tests were determined indirectly. These areas were then used with the slopes from the unloading curves to determine stiffness and elastic modulus as a function of indentation depth following the method of Oliver and Pharr (1992).

The resistance to interfacial fracture was determined using the same system configured to control normal loads and lateral indenter displacements. These tests employed a conical diamond indenter with a nominal 1µm tip radius and a 90° included angle that was simultaneously driven into the films at a loading rate of 500 µN/s and across the films at a rate of 0.5 µm/s until a portion of the film spalled from the substrate. During each test, the normal and tangential loads, the indenter depth, and the lateral position were continuously monitored. The fracture energy and interfacial fracture toughness values then were determined from the data using the elastic approach of Venkataraman et al. (1993) where the practical work of adhesion is defined as the total elastic strain energy released into the film and the substrate when the film delaminates. As a simple appproximation, Venkataraman et al. (1993) assumed that the extent of deformation in the film and substrate was similar and equated the strain energy released into the substrate to the strain energy released into the film as follows,

$$\Gamma_i = G_i = G_i^f + G_i^s = 2G_i^f = \sum\left(\frac{\bar{\tau}_{ij}^2}{2\mu}t + \frac{\bar{\sigma}_{ij}^2}{2E}t\right) \quad (1)$$

where Γ_i is the fracture energy or practical work of adhesion, G_i is the strain energy for interfacial fracture composed of the strain energy released upon fracture into the substrate, $G^s{}_i$, and into the film, $G^f{}_i$. The strain energy released into the film, $G^f{}_i$, is a function of the average

elastic shear, $\bar{\tau}_{ij}$, and normal stresses, $\bar{\sigma}_{ij}$, in the delaminated region. These stresses are determined from the critical normal and tangential loads at fracture, the area of delamination, the length of the delamination, the track width at the start of delamination, the shear modulus, µ, the elastic modulus, E, and the thickness of the film, t.

The resistance to fracture was also determined using the indentation method of Weppelmann, Hu, and Swain (1994) for hard films on softer substrates. In this method a conical diamond indenter with a one micron tip radius and 90° included angle was driven into the film at a rate of 300 µN/s to loads exceeding fracture. The film was assumed to behave elastically up to the first indication of fracture at which time a circular ring crack forms just outside the area of contact. The process was repeated as the load increased and was eventually followed by interfacial delamination. Displacement occurred not by deformation of the film but by substrate bending as the fractured film is pressed into the softer substrate. Assuming there are no residual stresses or any elastic mismatch, the maximum radial tensile stress driving the delamination crack is approximated as,

$$\sigma_{max} = \frac{(1-2\nu)}{2}\frac{P_c}{\pi a_c^2} \quad (2)$$

with a corresponding fracture energy for delamination of,

$$\Gamma_i = \frac{\sigma_{max}^2 t}{2E}\left(\frac{a_c}{c}\right)^2 \alpha \quad (3)$$

where,

$$\alpha = (\varepsilon_r/\varepsilon)^2 = (1-\delta_r/\delta)^2 \quad (4)$$

In these expressions, σ_{max} is the maximum radial tensile stress, P_c is the maximum load, a_c is the indentation radius, c is the delamination radius, t is the film thickness, and E is the film modulus. Because the indenter restricts film deflection after fracture, the strain energy release release rate is less than given by eq. (3) by a factor proportional to the square of the residual strain. This factor is defined as a function of residual displacement, δ_r, divided by displacement of the contact circle of the indenter, δ. (Weppelmann et al., 1994)

RESULTS AND DISCUSSION

The microstructure of both the polycrystalline aluminum nitride substrates and the tantalum nitride films were examined using SEM and TEM techniques. Both techniques detected yttrium-rich phases embedded in the aluminum nitride substrates. This result was expected as yttrium oxide is commonly added to aluminum nitride to improve both processing and heat transfer properties. The yttrium oxide can react to form several different yttrium aluminates. Our analyses have identified the presence of at least $Y_2O_3 \cdot Al_2O_3$ (yttrium aluminum Perovskite or YAP). Our initial analysis has detected no significant effect of these second phases on the structure of the tantalum nitride films.

Tantalum nitride can exist in several compositionally and structurally distinct forms. (Massalski et al., 1990) In the films of this study, scanning auger microscopy showed that the composition was constant with a two-to-one ratio between tantalum and nitrogen. However, the films exhibited two distinct microstructures even though they were deposited under nominally the same conditions. The structure of the 160-nm-thick film consisted of fine, nanometer-sized crystallites forming near the interface followed by 20-to-40-nm wide columnar grains, corresponding to individual crystallites extending to the surface of the film. (Fig. 1a) The columnar grains formed with a preferential [0002] crystal orientation parallel to the substrate

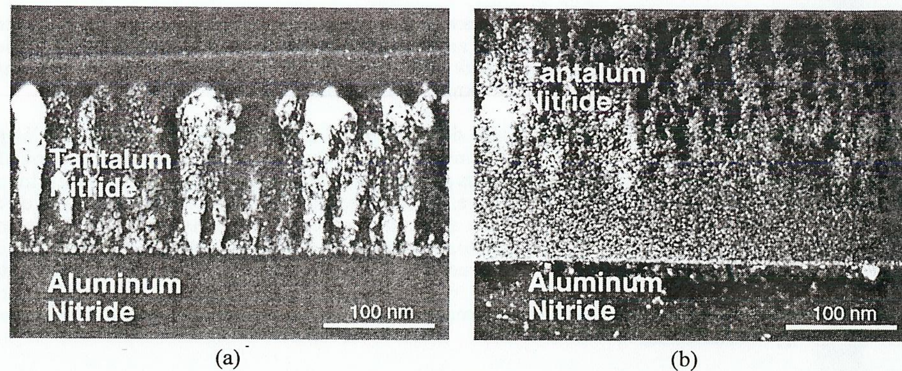

(a) (b)

Fig. 1. Dark field micrographs show that (a) the microstructure of 160-nm-thick films consisted of fine nanometer-sized crystallites along the film substrate interface and 20-to-40-nm-wide columnar grains extending through the film thickness. (b) The microstructure of the 440 and 500-nm-thick films consisted of an amorphous layer along the substrate interface followed by columnar grains extending to the surface.

normal as determined from electron diffraction analysis. Some fine-scale porosity was also identified along the columnar grain boundaries. In contrast, the structure of the 440 and 500-nm-thick films consisted of a 200-nm-thick amorphous layer near the interface followed by columnar grains extending to the surface. (Fig. 1b) The columnar grains also formed with a [0002] crystal orientation parallel to the substrate normal. The multilayer structure observed in the thicker films is often observed in tantalum nitride films deposited on oxide substrates. (Angelo et al., 1995; Au et al., 1990) Electron diffraction measurements identified the polycrystalline portions of the films in this study as Ta_2N in the trigonal form (space group $P\bar{3}1m$; lattice parameters: a=0.5255 nm and c=0.4919 nm). This structure consists of hexagonally close-packed tantalum atoms with interstitially distributed nitrogen.

Nanoindentation showed that the measured elastic moduli of all films were independent of indenter depth and approximately equal to the value measured for the aluminum nitride substrates as shown in Fig. 2a. In all these films, the measured values exhibited significant scatter within 50 nm of the film surface due in large part to variations in surface topology. Beyond 50 nm in depth the values exhibited little scatter. In contrast with the elastic property behavior, measured hardness values varied with indenter depth. The hardness values also increased with film thickness. Both effects are shown in Fig. 2b where the data for all films superimpose when plotted using the tantalum nitride-aluminum nitride interface as a common reference even though the microstructures of the films differ significantly. The superposition of elastic moduli and hardness values for all three films shows that film behavior does not depend on microstructure. With a constant composition and properties independent of microstructure, the intrinsic hardness of the films should be constant. The measured decrease in hardness can therefore be attributed to an increasing contribution from the softer substrate with increasing indenter depth.

A series of ten microscratch tests were run on each film to determine resistance to fracture. These tests showed that the critical loads for fracture increased from near 15 mN in 160-nm-thick films to 90 mN in 500-nm-thick films with the point of fracture characterized by an abrupt change in tangential load as shown in Fig. 3a. The fractures were always characterized by well-defined spalls along the film and substrate interface. (Fig. 3b) In all tests, the first spall provided the data needed to estimate elastic fracture energy and toughness. Compositional

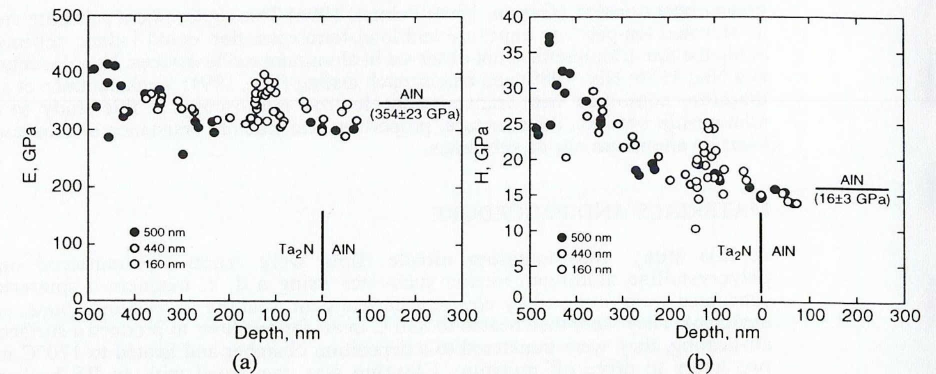

(a) (b)

Fig. 2. (a) The elastic moduli of all films were independent of indenter depth and approximately equal to the modulus of the AlN substrate. (b) The hardness values of all films superimposed, decreasing in value from the film surface to the AlN substrate.

scans across the fracture surface showed no evidence of tantalum from the film suggesting that fracture occurred along the interface or just within the aluminum nitride substrate. The measurement of normal and tangential forces provided a coefficient of friction equal to 0.28, which is significantly lower than the value of 0.63 for ductile grooving. (Venkataraman et al., 1993) The average elastic energies for fracture are given in Table I. This table shows that the average fracture energies values are essentially independent of film thickness.

Ten indentation fracture tests at maximum loads of either 200 or 250 mN and 400 mN were also run on the 440 and 500-nm-thick films. The response followed observations by Loubet et al. (1989) for TiN films on stainless steel and observations by Weppelmann et al. (1994) for TiN on Silicon. At low loads the indentation curve is elastic and reversible. At higher loads there are small breaks and excursions in the load-displacement curve. (Fig. 4a) SEM shows that these breaks most likely arise from formation of annular cracks beneath the indenter. As the loads increased radial cracks formed with partial spalling providing clear evidence that these cracks accompany delamination with no evidence for buckling or buckling-driven delamination. (Fig. 4b)

Although AlN is hard in comparison to most materials, it is softer than tantalum nitride. As a consequence, tantalum nitride behaves as a hard film on a soft substrate. This behavior is readily apparent in Fig. 4b where the film under the indenter has been forced into the substrate. However, since AlN has a low strength to modulus ratio, any plastic deformation is confined to well within the region beneath the indenter. (Bolshakov and Pharr, 1996) The maximum radial

Table I. Elastic fracture energies, Γ_i, along with average areas of spallation, A, critical normal and tangential loads at failure, P_{cr} and L_{cr}, film thickness, t, and elastic modulus, E, from scratch tests of thin tantalum nitride films on polished polycrystal aluminum nitride substrates.

t (nm)	A (μm^2)	P_{cr} (mN)	L_{cr} (mN)	E (GPa)	Γ_i (J/m^2)
160	8±2	16±4	6±2	350	0.4±0.2
440	81±33	78±14	23±5	350	0.4±0.3
500	99±22	90±12	25±7	350	0.5±0.2

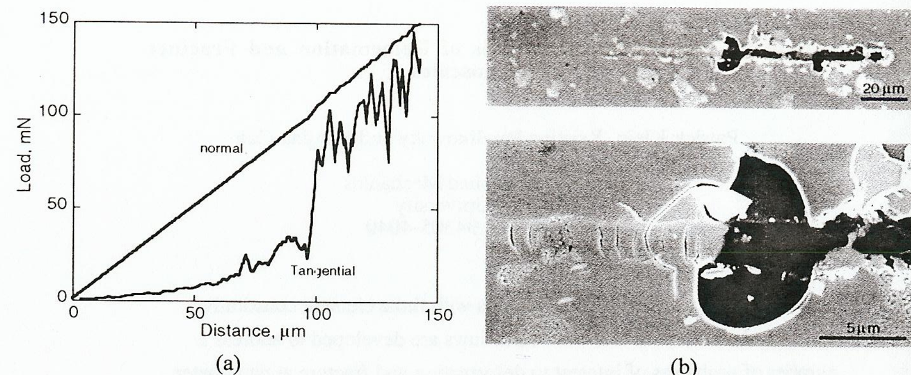

Fig. 3. Tantalum nitride films on aluminum nitride substrates (a) consistently failed at normal loads near 80 mN for 440-nm-thick films and were accompanied by (b) well-defined spalls along the film and substrate interface.

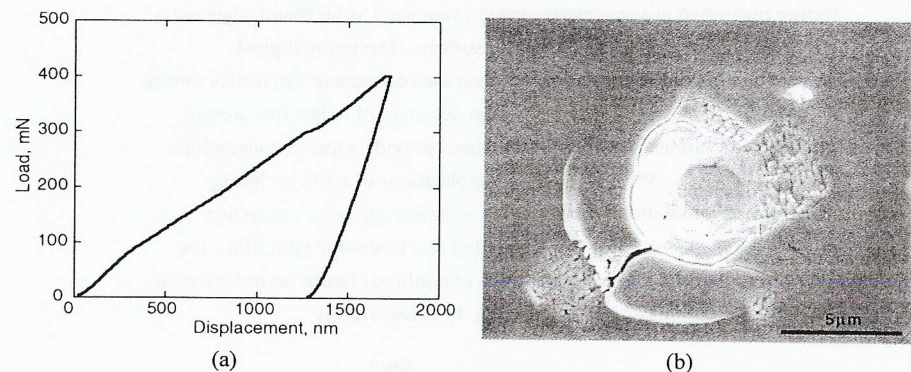

Fig. 4. Delamination during indentation is characterized by (a) small breaks and excursions in the load-displacement curve. The corresponding fracture (b) clearly shows the film has been pushed into the substrate under the indenter with delamination emanating from the impression.

tensile stress driving delamination can therefore be approximated by the maximum applied load acting over the contact area given by eq. (2). Residual displacement is determined from the sum of the depth excursions in the load-displacement curves (Weppelmann et al., 1994) and the actual displacement is given by the elastic deflection of the contact circle. (Oliver and Pharr, 1992) The average elastic energies for indentation fracture, Γ_i, were then calculated from these values using eq. (3) and (4) and are given in Table II. These values compare surprisingly well with values from the scratch test given in Table I.

The measured fracture energies are at the upper end of van der Waals forces and are consistent with observations showing that sputtered films adhere more strongly to substrates than evaporated films. (Chopra, 1969) The energies are also more than a factor of two lower than than the energies associated with metallic bonding. When combined with the observations that fracture is localized to the film-substrate interfaces and occurred at fracture energies that are independent of film thickness and microstructure, the results strongly suggest that as-sputtered tantalum nitride films on aluminum nitride substrates form a near perfect brittle film system. The results further suggest that bond formation between the tantalum nitride film and the aluminum oxide interfacial layer on the aluminum nitride substrate controls adhesion.

Table II. Elastic fracture energies, Γ_i, along with film thickness, t, average radius of indentation, a_c, average radius of delamination, c, maximum applied normal load, P_{cr}, and elastic modulus of the film, E, from indentation fracture of thin tantalum nitride films on polished polycrystal aluminum nitride substrates.

t (nm)	a_c (µm)	c (µm)	P_{cr} (mN)	E (GPa)	Γ_i (J/m^2)
440	1.7±0.1	4.0±0.8	250	350	1.0±0.4
440	2.3±0.1	5.7±0.8	400	350	0.5±0.3
500	2.0±0.1	3.4±0.5	200	350	0.2±0.1
500	2.4±0.1	7.2±1.6	400	350	0.4±0.3

SUMMARY

Nanoindentation and nanoscratch testing were used in this study to determine the relationship between microstructure and properties for thin tantalum nitride films on polished polycrystalline aluminum nitride substrates. These films were sputter-deposited to nominal thicknesses of 160, 440, and 500 nm. The structure of these films consisted of fine equiaxed crystallites along the film-substrate interfaces and long columnar grains extending to the film surface with only fine scale porosity along the columnar grain boundaries. The elastic moduli were independent of thickness and approximately equal to the modulus of the aluminum nitride substrate of 350 GPa. In contrast, measured hardness decreased from relatively high values of 35 GPa at the surface of the 500-nm-thick film to aluminum nitride values at the substrate. The fracture energies measured using nanoscratch and nanoindentation fracture techniques were essentially equal and independent of film thickness even though the microsctructures differed. The results showed that fracture was localized to the film-substrate interface and strongly suggest that adhesion was controlled by the nature of bonding across the interface plane.

ACKNOWLEDGMENTS

The authors thank C. Rood, M. Clift, and D. Boehme from Sandia National Laboratories, Livermore, CA for their technical support and D. Bahr from the University of Minnesota for helpful discussions. The authors also acknowledge the support of the U.S. DOE through Contract DE-AC04-94AL85000.

REFERENCES

Angelo, J. E., N. R. Moody, S. K. Venkataraman, and W. W. Gerberich (1995). Effects of annealing on the structure of Ta_2N thin films deposited on Al_2O_3, In *Structure and Properties of Defects in Ceramics*, vol. **357** (D. A. Bonell, M. Ruhle, and U. Chowdhry, eds.) pp. 195-200, MRS, Pittsburgh, PA.

Au, C. L., W. A. Anderson, D. A. Schmitz, J. C. Flassayer, and F. M. Collins (1990). Stability of tantalum nitride thin film resistors, *J. Mater. Res.*, **5** , 1224-1232.

Bolshakov, A. and G. M. Pharr, (1996). to be published, Rice University, Houston, TX.

Chopra, K. L. (1969). *Thin Film Phenomena.* McGraw-Hill Book Co., New York.

Doerner, M. F. and W. D. Nix (1986). A method for interpreting the data from depth-sensing indentation instruments, *J. Mater. Res.*, **1**, 601-609.

Evans, A. G. and J. W. Hutchinson (1984). On the mechanics of delamination and spalling in compressed films, *Int. J. Solids Structures*, **20**, 455-466.

Garrou, P. (1994). Aluminum nitride for microelectronic packaging, *Advancing Microelectronics*, **21**, 6-10.

Loubet, J. L., J. M. Georges, and Ph. Kapssa, (1989). Measurement of thin film adhesion and mechanical properties with indentation curves. In *Mechanics of Coatings* (D. Dawson, ed.) pp.429-434, Elsevier, New York.

Massalski, T. B. ed. (1990). *Binary Alloy Phase Diagrams*. 2nd Edition, ASM International, Metals Park, OH.

Mittal, K. L. (1976). Adhesion measurement of thin films, *Electrocomponent Science and Technology*, **3**, 21-42.

Nix, W. D. (1989). Mechanical properties of thin films, *Metall. Trans. A*, **20A**, 2217-2245.

Oliver, W. C. and G. M. Pharr (1992).An improved technique for determining hardness and elastic modulus, *J. Mater. Res.*, **7**, 1564-1583.

Palmer, R. H. (1994). The Use of AlN in semiconductor packaging at motorola, *Advancing Microelectronics,* **21**, 11-14.

Rickersby, D. S. (1988). A review of the methods for the measurement of coating-substrate adhesion, *Surface and Coatings Technology*, **36**, 541-557.

Venkataraman, S. K., D. L. Kohlstedt, and W. W. Gerberich (1993). Microscratch analysis of the work of adhesion for Pt thin films on NiO, *J. Mater. Res.*, **7**, 1126-1132.

Weppelmann, E. R., X.-Z. Hu, and M. V. Swain, (1994). Observations and simple fracture mechanics analysis of indentation fracture delamination of TiN films on silicon, *J. Adhesion Science and Technol.*, **8**, 611-624.

Wu, T. W. (1991). Microscratch and load relaxation tests for ultra-thin films, *J. Mater. Res.*, **6**, 407-426.